HAL open science

Theoretical analysis of the effect of the interfacial MoSe_2 layer in CIGS-based solar cells

Adama Sylla, N'guessan Armel Ignace, Touré Siaka, Jean-Pierre Vilcot

To cite this version:

Adama Sylla, N'guessan Armel Ignace, Touré Siaka, Jean-Pierre Vilcot. Theoretical analysis of the effect of the interfacial MoSe_2 layer in CIGS-based solar cells. Open Journal of Modelling and Simulation, 2021, 09 (04), pp.339-350. 10.4236/ojmsi.2021.94022 . hal-03681482

HAL Id: hal-03681482

https://hal.science/hal-03681482v1

Submitted on 2 Jun 2022

HAL is a multi-disciplinary open access archive for the deposit and dissemination of scientific research documents, whether they are published or not. The documents may come from teaching and research institutions in France or abroad, or from public or private research centers.

L'archive ouverte pluridisciplinaire **HAL**, est destinée au dépôt et à la diffusion de documents scientifiques de niveau recherche, publiés ou non, émanant des établissements d'enseignement et de recherche français ou étrangers, des laboratoires publics ou privés.

Distributed under a Creative Commons Attribution 4.0 International License

Open Journal of Modelling and Simulation, 2021, 9, 339-350
https://www.scirp.org/journal/ojmsi
ISSN Online: 2327-4026
ISSN Print: 2327-4018

Theoretical Analysis of the Effect of the Interfacial $MoSe_2$ Layer in CIGS-Based Solar Cells

Adama Sylla[1], N'Guessan Armel Ignace[1], Touré Siaka[1], Jean-Pierre Vilcot[2]

[1]Laboratoitre d'Energie Solaire, Université Félix Houphouët Boigny, Abidjan, Côte d'Ivoire
[2]Institut d'Electronique, de Microélectronique et de Nanotechnologie (IEMN), UMR, CNRS, 8520. Laboratoire Central, Villeneuve d'Ascq Cedex, Lille, France
Email: sylla_adama1959@yahoo.fr

How to cite this paper: Sylla, A., Ignace, N.A., Siaka, T. and Vilcot, J.-P. (2021) Theoretical Analysis of the Effect of the Interfacial $MoSe_2$ Layer in CIGS-Based Solar Cells. *Open Journal of Modelling and Simulation*, **9**, 339-350.
https://doi.org/10.4236/ojmsi.2021.94022

Received: July 20, 2021
Accepted: August 27, 2021
Published: August 30, 2021

Copyright © 2021 by author(s) and Scientific Research Publishing Inc.
This work is licensed under the Creative Commons Attribution International License (CC BY 4.0).
http://creativecommons.org/licenses/by/4.0/
Open Access

Abstract

The aim of this work is to analyze the influence of the interfacial $MoSe_2$ layer on the performance of a /n-ZnO/i-ZnO/n-Zn(O,S)/p-CIGS/p^+-$MoSe_2$/Mo/SLG solar cell. In this investigation, the numerical simulation software AFORS-HET is used to calculate the electrical characteristics of the cell with and without this $MoSe_2$ layer. Different reported experimental works have highlighted the presence of a thin-film $MoSe_2$ layer at the CIGS/Mo contact interface. Under a tunneling effect, this $MoSe_2$ layer transforms the Schottky CIGS/Mo contact nature into a quasi-ohmic one. Owing to a heavily p-doping, the $MoSe_2$ thin layer allows better transport of majority carrier, tunneling them from CIGS to Mo. Moreover, the bandgap of $MoSe_2$ is wider than that of the CIGS absorbing layer, such that an electric field is generated close to the back surface. The presence of this electric field reduces carrier recombination at the interface. Under these conditions, we examined the performance of the cell with and without $MoSe_2$ layer. When the thickness of the CIGS absorber is in the range from 3.5 μm down to 1.5 μm, the efficiency of the cell with a $MoSe_2$ interfacial layer remains almost constant, about 24.6%, while that of the $MoSe_2$-free solar cell decreases from 24.6% to 23.4%. Besides, a Schottky barrier height larger than 0.45 eV severely affects the fill factor and open circuit voltage of the solar cell with $MoSe_2$ interface layer compared to the $MoSe_2$-free solar cell.

Keywords

CIGS, Numerical Simulation, AFORS-HET, Quasi-Ohmic Contact, Schottky Contact, $MoSe_2$, Tunnel Layer

1. Introduction

High efficiency CIGS-based solar cells have been the focus of several years of theoretical and experimental research. The recent high laboratory efficiency values of 22.9% and 23.4% (Solar Frontier) [1] [2] are close to the efficiency of 25% achieved by crystalline silicon solar cells. These thin-film cells have achieved the best performance of all second-generation cell technologies. The current achieved efficiency is the result of the technological advances which allow the efficiency to be improved empirically by successive tests. In addition to the technological progress observed over the last two decades, significant efforts have been devoted to understanding the physical properties of the key material of these cells, namely the CIGS absorber layer. Indeed, the performance of these cells largely depends on the physical properties of the CIGS alloys which are not yet fully clarified. These include the nature and energy levels of the CIGS absorbing layer defects and the buffer/absorber interface defects [3] [4]. Moreover, data about the material's properties strongly depend on the used growth process and characterization techniques [3] [4]. This entails input parameters of simulation works may vary within wide ranges, imposing some limitation on the accuracy of simulated results. However, CIGS (namely $CuIn_{1-x}Ga_xSe_2$) material remains one of the most promising semiconductor materials for photovoltaic conversion based on polycrystalline thin-films because of several favorable properties:

1) Its bandgap can be varied continuously by changing the gallium content, *x*, and its value is given by the commonly used formula (all bandgap energies in eV) [5] [6] [7]:

$$E_{gCI_{1-x}G_xS} = (1-x)\cdot E_{gCIS} + x\cdot E_{gCGS} - b\cdot x\cdot(1-x).$$

where b is the bowing parameter, E_{gCGS}, E_{gCIS}, the bandgaps of CGS and CIS ternary compounds, respectively. Due to above-mentioned concerns, the value of the bowing parameter can vary in the 0.15 - 0.24 eV range and that of E_{gCGS} and E_{gCIS} in between 1.63 - 1.67 eV and 1.01 - 1.05 eV, respectively. We chose here $b = 0.21$ eV, $E_{gCGS} = 1.65\,\text{eV}$ and $E_{gCIS} = 1.04\,\text{eV}$ [5]. All values are given at 300˚K.

2) The commonly referred surface defect layer (SDL), that is present between the absorber and buffer layers increases the absorber bandgap at this interface by lowering the valence band maximum with respect to the Fermi level, and hence reduces the interface recombination rate. In fact, it has been found that this surface defect layer is inverted to n-type such that the photogenerated electrons pass through this region as majority carriers.

3) CIGS is a direct bandgap alloy with an absorption coefficient that can reach 10^5 to 10^7 cm^{-1}, here too depending on its fabrication process, so that a thin thickness of 0.5 µm is sufficient to absorb 90% of the incident photon flux [3].

4) Unlike silicon, CIGS materials have exceptional tolerance to structural and chemical defects

On the other hand, the high cost and low abundance of indium and gallium

remains, in the long term, a major concern as well as the relatively significant degradation of performance observed in case of long-term exposure to the atmosphere, which requires appropriate encapsulation. However, technological progress has made it possible to produce cells with high efficiencies where the usual CdS buffer layer is replaced by cheap and better eco-friendly materials as ZnS, ZnO, and the ternary compound $ZnO_{1-x}S_x$. This latter is the most promising material with a variable bandgap from 3.6 eV to 3.2 eV [8] [9] [10].

Thin-film cells have nevertheless a small market share compared to their silicon counterparts but, in recent years, they have risen sharply mainly focusing on their particular asset allowing the fabrication of flexible cells. Several routes have been explored to fabricate them on metal and plastic foils jointly enhancing their conversion efficiency by reducing sufficiently the photogenerated carrier recombination caused by the bulk defects. The ultimate goal is affording the flexibility with efficiencies and lifetime comparable to that of rigid cells.

One approach to decrease the raw material cost is to reduce drastically the thickness of the absorber. In that case, the carrier photogeneration rate close to the back contact can no more be negligible and the recombination rate at the back interface is of prime importance. Another approach is to create an electric field within the CIGS absorber by bandgap grading located at appropriate regions. This results in various cell structures with different CIGS composition profiles: the so-called "front grading" which has a higher bandgap towards the buffer layer, "back grading" which has a higher bandgap towards the back contact layer and "double grading" which combines the two first profiles of grading. Thus, front grading reduces recombination at the buffer/absorber junction and back grading does close to the backside pushing back minority carriers towards the collecting junction, then reducing carrier recombination at the absorber backside [11].

Many metals have been studied for contacting the photovoltaic cells to the external circuit. Mention may be made of molybdenum, chromium, tantalum, manganese, gold and silver [12] [13]. Among those, the molybdenum is widely used as back contact metal because of its relative stability at the high temperatures that are encountered during CIGS deposition steps and its low contact resistance with CIGS [14]. Its work function is about 4.53 eV [15]. In addition, the existence of a thin $MoSe_2$ layer at the CIGS/Mo interface has been clearly demonstrated to improve the adhesion of CIGS to Mo as well as to enhance the efficiency of the cell [14] [15] [16] [17]. $MoSe_2$ is a semi-conductor material with a bandgap of about 1.41 eV.

Lots of experimental studies have been carried out on the role of the $MoSe_2$ layer at the interface of the CIGS/Mo contact of cells that use a CdS buffer to achieve the p-n junction [18] [19] [20]. However, the formation of the thin $MoSe_2$ layer depends on the fabrication process (deposition technique of CIGS, associated temperatures…) that is used to realize the cell [18].

Several authors demonstrated the remarkable technological advantages of Mo. But they also demonstrated the low reflexivity at the CIGS/Mo interface, which

has a negative impact on the thin-film CIGS solar cells performance (reduction of the short circuit current and the open circuit voltage). The aim of our work is to determine the real contribution of the CIGS/Mo contact to the cell performance through the $MoSe_2$ thin layer presents at the CIGS/Mo interface. In this paper, a ZnS buffer is used and we theoretically examine how the $MoSe_2$ layer influences the CIGS solar cell performance. For that purpose and after the optimization of a $MoSe_2$-free solar cell, we investigate successively the effects of the CIGS and $MoSe_2$ layer thickness and the barrier height of the Schottky $MoSe_2$/Mo back contact.

2. Numerical Simulation

In [3] [4], we reported the optimizing of CIGS-based solar cell including a $MoSe_2$ layer at the CIGS/Mo interface. The values of front and back contact reflectivity were set to 0% and the front and backside boundaries of the stacked semi-conductors were described by the flat band metal/semi-conductor contact model. Under those conditions, we demonstrated a maximum conversion efficiency of 26% [3].

Here, we use AFORS-HET to carry out the simulation work [21]. The simulation of the $MoSe_2$-free solar cell is based on Fermi level pinning model. The values of the optimized parameters are extracted from our previous papers [3] [4] and take into account the Schottky barrier height at the back contact and the reflectivity on the front (illuminated) side (**Figure 1**). The input parameters of AFORS-HET simulation are listed in **Table 1** and **Table 2**.

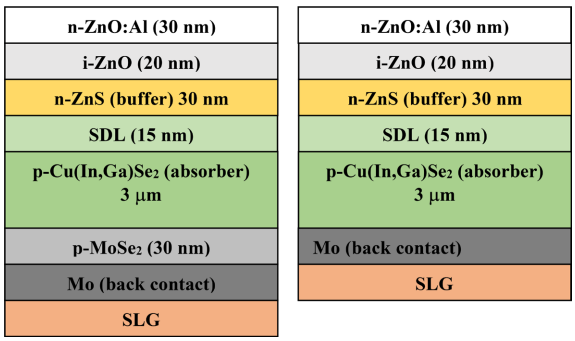

Figure 1. Schematic configuration of the optimized CIGS-based solar cell (a) with and (b) without $MoSe_2$ layer.

Table 1. Device properties: Subscripts n and p refer to electron and hole properties, respectively, E_B to majority carrier barrier height ($E_{Bn} = E_C - E_F$, $E_{Bp} = E_F - E_V$) and $S_{n,p}$ to back surface recombination velocity.

	Front side	Back side
E_{Bn}/E_{Bp} (eV)	0.02	0.3
S_n (cm/s) S_p (cm/s)	10^7	10^7
Reflectivity (R)	5%	0%

Table 2. Layer properties values used in AFORS-HET simulation: $S_{th}^{n,p}$ refers to carrier thermal velocity, $\mu_{n,p}$ to carrier mobility, E_g to bandgap energy, N_C/N_V to effective density of states in conduction and valence bands, (a)/(d) shallow acceptor and donor, and $\Delta E_C/\Delta E_V$ to band offset.

	Layers properties					
	$MoSe_2$	**CIGSe**	**ZnS**	**ZnS**	**i-ZnO**	**ZnO:Al**
Thickness (μm)	0.01	variable	0.015	0.03	0.02	0.03
Band gap E_g (eV)	1.41	1.19	1.34	3.6	3.2	3.2
Electron affinity χ (eV)	4.4	4.5	4.5	4.15	4.5	4.5
Dielectric constant ε_r	14.9	13.6	13.6	9	9	9
N_C (cm^{-3})	2.2×10^{18}	6.8×10^{17}	6.8×10^{17}	2.2×10^{18}	3×10^{18}	3×10^{17}
N_V (cm^{-3})	1.8×10^{18}	1.5×10^{19}	1.5×10^{19}	1.8×10^{19}	1.7×10^{19}	1.7×10^{19}
S_{th}^{n}, S_{th}^{p} (cm/s)	10^7					
μ_n (cm^2/Vs)	100	100	10	100	100	100
μ_p (cm^2/Vs)	50	50	1.25	25	31	31
Doping level (cm^{-3})	10^{19} (a)	6×10^{17} (a)	6×10^{17} (a)	10^{18} (d)	10^{18} (d)	10^{20} (d)
	$MoSe_2$/CIGS	**CIGS/SDL**	**SDL(CIGS)/ZnS**			**ZnS/i-ZnO**
ΔE_C (eV)	0.1	0	0.35 (0.35)			−0.35
ΔE_V (eV)	−0.12	−0.15	−1.19 (−2.06)			0.05

Contrary to our previously reported simulation, the reflectivity at front side is $R = 5\%$ and the back Schottky barrier height $E_B = 0.3$ eV is higher than that previously used ($E_B \approx 0.02$ eV) [3] [4]. The Schottky barrier height is deduced from the formula $E_B = \chi + E_g - \Phi_{Mo}$ where χ and E_g denote respectively the electronic affinity and the bandgap of the semi-conductor material in contact with Mo and Φ_{Mo} the work function of molybdenum. AFORS-HET uses the Shockley-Read-Hall recombination model and solves the fundamental one-dimensional semiconductor equations for steady-state equilibrium conditions under solar illumination [21]. The metal-semiconductor contact simulation is implemented according to the metal work function. Therefore, the contact can operate either in flat band mode or in band bending mode. AFORS-HET simulator allows the calculation of basic characteristics such as band diagram, generation and recombination rates, carrier densities and cell currents [21].

The simulated cell structures consist of six or seven stacked layers, depending the p-$MoSe_2$ layer is absent or present, respectively (see **Figure 1**). These layers are deposited on a soda lime glass (SLG) substrate. Only the front contact boundaries of the solar cells are described by the flat band metal/semiconductor contact model. The solar cell front side is illuminated under AM1.5G solar spectrum corresponding to an incident power density of 100 mW/cm^2 at room temperature (1 Sun). Under these conditions, we calculated the effects of the thickness of the CIGS and $MoSe_2$ layers that varied from 0.1 μm to 10 μm and from 10 nm to 100 nm respectively. As for the Schottky barrier height at the back $MoSe_2$/Mo contact it has been varied from 0.2 eV to 0.65 eV according to the work function

of molybdenum that was tuned from 5.16 eV to 5.61 eV.

3. Results and Discussion

3.1. Solar Cell Optimization

The thickness of each layers of the solar cells, including or not the $MoSe_2$ layer, has been optimized. The conversion efficiency obtained for the $MoSe_2$-free solar cell η = 24.6% is equal to that of the cell including a $MoSe_2$ thin-film layer at the CIGS/Mo contact interface. This value of efficiency has been obtained for a 3 µm-thick CIGS absorber with a front side reflectivity of 5%. The Schottky barrier height is 0.3 eV and 0.18 eV for the solar cells with and without $MoSe_2$ layer respectively.

The mechanism of carrier transport in metal/semi-conductor contact is intimately related to the energy band structure at the interface under thermodynamic equilibrium conditions. We therefore examined in the next paragraphs the real electrical impact of the $MoSe_2$/Mo contact on CIGS solar cell performance. Our approach consisted in modifying the Schottky barrier height at the interface of CIGS/Mo and $MoSe_2$/Mo intimate contacts of the two cells structure and varying the $MoSe_2$ and CIGS layers thickness, the other parameters being kept constant.

3.2. Effect of the $MoSe_2$ Layer Thickness on Internal Quantum Efficiency (IQE)

To analyze the effect of the $MoSe_2$ layer thickness on the IQE (or η), we varied its value from 10 to 100 nm (**Figure 2**). We can see that for $MoSe_2$ layer thickness larger than 30 nm the cell efficiency remains almost constant. So, the $MoSe_2$ layer thickness was set at 30 nm for the other studies. The photocarrier recombonation is considerable at the CIGS/Mo contact interface. The presence of the $MoSe_2$ layer with a relatively large thickness (30 nm) moves this zone of recombination away from the CIGS absorber layer. Under these conditions the tunnel effet outweighs the recombination and improves the efficiency.

3.3. Effect of the $MoSe_2$ Layer on the External Quantum Efficiency (EQE)

The EQE expresses the flow of electrons through the external circuit of use

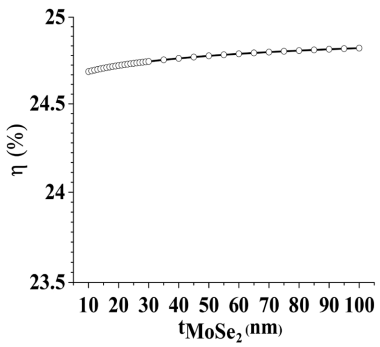

Figure 2. Effect of the $MoSe_2$ layer thickness on the cell efficiency (absorbing layer thickness is of 3 µm).

according to the wavelength absorbed. Compared to IQE, it takes into account two important factors that are optical losses and photocarrier recombinations. For the large absorber thicknesses ($t_{CIGS} \geq 3$ µm), the EQE is almost identical for both structures, with and without $MoSe_2$ layer. On the other hand, for CIGS thicknesses less than 3 µm, the EQE of the solar cell with a $MoSe_2$ layer is higher. We have plotted the EQE curves for a solar cell including a 1.5 µm thick CIGS absorbing layer with and without the $MoSe_2$ layer (30 nm thick). **Figure 3** shows that the cell including the $MoSe_2$ layer offers a higher EQE value in the long wavelength range compared to the $MoSe_2$-free cell.

3.4. Effet of CIGS Layer Thickness on the Electrical Parameters

In order to investigate the effect of the absorber layer thickness on the electrical parameters of cells with and without a $MoSe_2$ layer, we varied the CIGS thickness from 0.1 to 10 µm. The photovoltaic performance of cells including a $MoSe_2$ layer are better than that of the $MoSe_2$-free solar cell (**Figure 4**) But this enhancement only appears for absorber thickness less than 3.5 µm, that is at least the majority, if not all, of experimental cases. For higher thickness values the performance of the two kinds of cells are almost identical: the efficiency increases up to about 25% with a slope of around 0.1% per additional micron of layer thickness (**Figure 4(a)**). It can also be observed that the efficiency of the cell with a $MoSe_2$/Mo back contact remains almost constant, about 24.6% down to an absorber layer thickness of 1.5 µm, while that of the $MoSe_2$-free cell decreases from 24.6% to 23.4% in the same range. So, the efficiency of the cell with a $MoSe_2$ layer is more independent on the absorbing layer thickness since it starts to decrease when CIGS thickness is less than 1.5 µm, while that of the $MoSe_2$-free cell starts to decrease at approximately 3.5 µm. For CIGS layer thickness less than approximately 0.5 µm, the effciency decreases rapidly in both cases because the carrier generation occurs very close to the back side where the carrier recombination is considerable. It can be seen in **Figure 4(d)** that the short circuit current presents a similar evolution than efficiency over the whole range of the absorber thickness variation. Looking now at FF in **Figure 4(b)**, we observe that the fill factor of the cell with $MoSe_2$ layer remains almost unchanged, whatever the

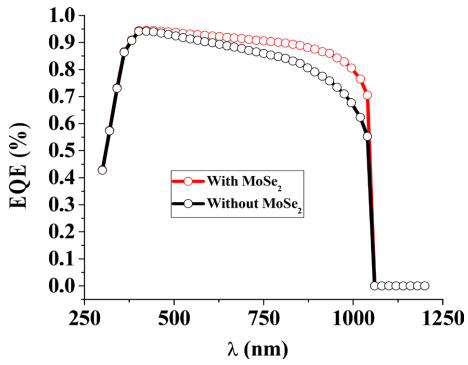

Figure 3. Effect of $MoSe_2$ layer (30 nm thick) on the EQE (absorber thickness is of 1.5 µm).

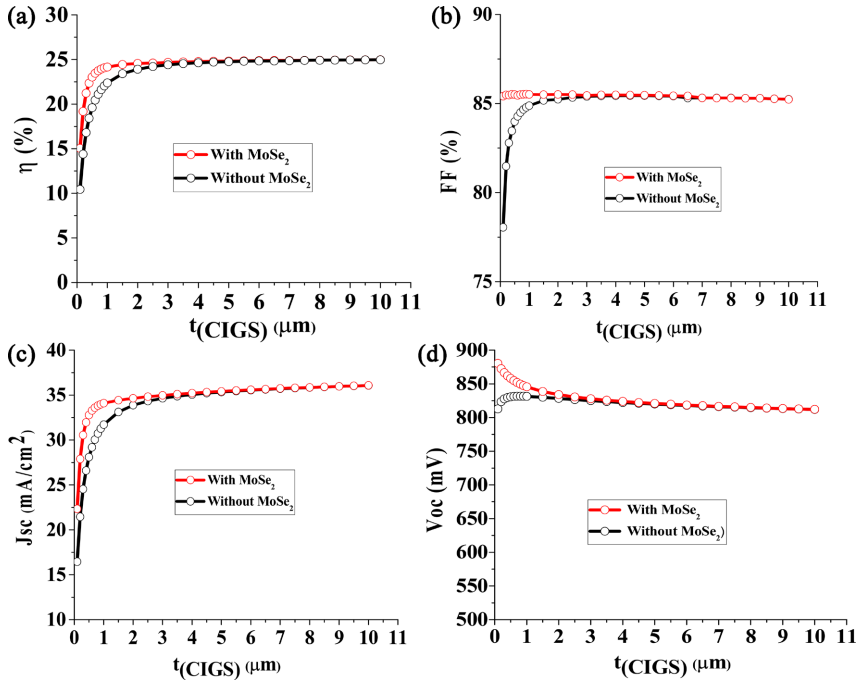

Figure 4. Effects of absorber layer thickness on cell performance for cell with and without $MoSe_2$ layer (30 nm thick). (a) conversion efficiency η, (b) fill factor FF, (c) open circuit volatge V_{OC} and (d) short circuit current J_{SC}.

thickness of the absorber is. On the over hand, for the $MoSe_2$-free solar cell, the fill factor starts decreasing at a switchover point of 3.5 μm. A similar evolution of the open circuit voltage is observed for absorber layer thickness higher than 3.5 μm. For the solar cell including the $MoSe_2$ layer, an increase of the open circuit voltage is observed for lowest thickness values of the CIGS absorbing layer (**Figure 4(c)**, $t_{CIGS} < 3.5$ μm) since it is almost the reverse case for the $MoSe_2$-free cell.

To get a deeper insight into the better performance of the thinner CIGS solar cell with a $MoSe_2$/Mo layer, we analysed more deeply the band structure (**Figure 5**). Under maximum effciency conditions, *i.e.* the work function of Mo, p-CIGS and p^+-$MoSe_2$ are $e\phi_{Mo} = 5.51$ eV, $e\phi_{SC1} = 5.61$ eV and $e\phi_{SC2} = 5.8$ eV, respectively (other values of parameters are that of **Figure 1**), $e\phi_{SC1}$ and $e\phi_{SC2}$ always remain greater than $e\phi_{Mo}$ and the CIGS/Mo and $MoSe_2$/Mo intimate contacts are of Schottky-type. However, unlike the $MoSe_2$-free cell, the highly p-doped $MoSe_2$ layer improves the majority carrier flow at the CIGS/Mo interface by tunneling effect. This tunnel barrier effect changes the intimate CIGS/Mo contact from Schottky type to quasi-ohmic type. Therefore the $MoSe_2$ layer has the ability to improve the generated carrier collection and increase the open circuit voltage and the conversion efficiency. In fact, the $MoSe_2$ layer has a wider gap than that of the absorber, then creating a back electric field that considerably reduces recombination at the CIGS back side. Furthermore, at the CIGS/$MoSe_2$ interface the conduction band also exhibits a spike that contributes to the reduction of the CIGS back surface recombination losses by reflecting the photogenerated electrons back to the junction where they are collected efficiently.

3.5. Effet of Schottky Barrier Height at the Back Contact Interface

To investigate the effect of the Schottky barrier height at the CIGS/Mo contact interface, we varied the metal work function from 5.16 to 5.61 eV for $MoSe_2$-free and $MoSe_2$/Mo contacts (Figure 6). As far as the metal work function $\Phi_{Mo} \geq 5.36$ eV, *i.e.* the Schottky barrier height is less than 0.45 eV (work function of p^+-$MoSe_2$, $e\phi_{SC2}$, is 5.8 eV), the electrical characteristics (efficiency, fill factor,

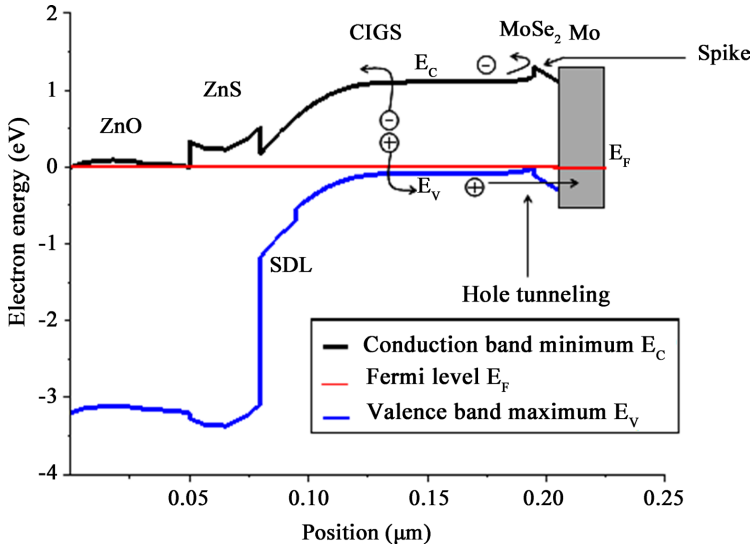

Figure 5. Calculated band structure of the CIGS solar cell with additional $MoSe_2$ layer under zero-bias voltage.

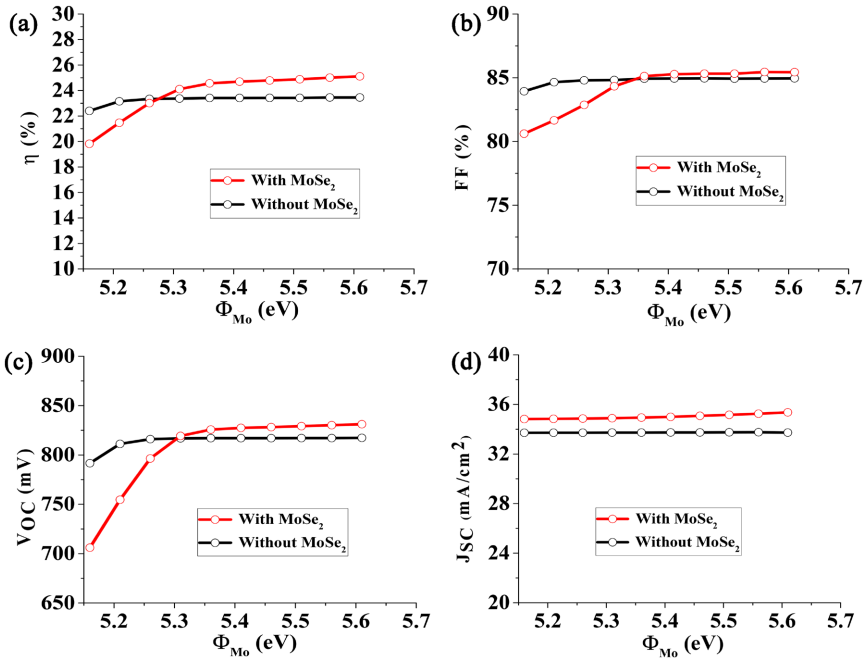

Figure 6. Effects of the Schottky barrier height on cell performance for $MoSe_2$-free cell and cell with additional $MoSe_2$ layer. (a) conversion efficiency η, (b) fill factor FF, (c) open circuit volatge V_{OC} and (d) short circuit current J_{SC}. (absorbing layer thickness is 1.5 µm).

open circuit voltage) of the cell with a $MoSe_2$ tunnel layer are better than those of the $MoSe_2$-free cell. However, related values increase slightly with the increase of the metal work function value. Whatever Φ_{Mo} value is, the short circuit current is higher for the $MoSe_2$ cell. In fact, the $MoSe_2$ tunnel layer eliminates the blocking effect of the Schottky barrier height to the flow of holes. In contrast, for $\Phi_{Mo} \leq$ 5.36 eV, the barrier height becomes prohibitive ($E_B \geq 0.45$ eV) and a pronounced degradation of the conversion efficiency, open circuit voltage and fill factor values is observed. They are then below that of a $MoSe_2$-free cell. For the investigated metal work function range, the barrier height at the intimate CIGS/Mo contact interface is relatively low and decreases from 0.53 to 0.08 eV. In this range of barrier height values, each of them is related to a metal work function value via the formula of Section II. So, the decrease of the barrier height from 0.53 eV to 0.08 eV corresponds to an increase of the metal work function value from 5.16 eV to 5.61 eV. The performance of the $MoSe_2$-free cell remains low but almost constant and the negative effect of the Schottky barrier height is only observed for values greater than 0.43 eV. In conclusion, it is the quasi-ohmic nature of the $MoSe_2$/Mo contact and the reduction of the CIGS back surface recombination rate that increase the open circuit voltage, the fill factor and the conversion efficiency as it has been demonstrated by other authors [18] [20].

4. Conclusions

This article focused on the comparative theoretical study, using AFORS-HET software, of two kinds of CIGS-based solar cells performance differentiating by the presence of a $MoSe_2$ layer at the CIGS/Mo interface. Overall conclusion is that the performance of a cell including such a $MoSe_2$ layer is better than that of the $MoSe_2$-free cell. Its thickness does not seem to be very challenging; 30 nm can be a suitable value. The $MoSe_2$ layer, firstly, acts as a tunneling barrier providing a quasi-ohmic back contact behavior and, secondly, creates a back surface electric field owing to its wider bandgap than that of CIGS absorber. However, to achieve such a behavior, the molybdenum work function shall be higher than 5.36 eV. These improvements are valid only for absorbing layer thickness less than 3.5 μm that constitute all practical cases, though. Moreover, the $MoSe_2$ layer beneficial effect is all the more important as the absorbing layer is thin, especially below 1 μm. Under those conditions, cells including a $MoSe_2$ tunnel layer can theoretically exhibit an efficiency of about 24.6%.

The model studied in this work has two junctions: the n-Zn (O, S)/n-SDL isotype heterojunction and the n-SDL/p-CIGS homojunction buried in the CIGS absorber layer (buried junction). Under these conditions, the n-Zn (O, S)/p-CIGS heterojunction raises several questions, in particular the advantage of the buffer which does not really form the collecting junction with the CIGS absorber layer, the density and the influence of defects at the interface of the homo- and heterojunction as well as the maximum efficiency achievable. In perspective, we plan to study the doping model where the surface defect layer (SDL) of the CIGS ab-

sorber is considered to be a chalcopyrite-like n-doped material with a bandgap higher than that of CIGS. These calculations could be carried out with the SCAPS-1D software package widely used for the simulation of CIGS-based heterojunctions.

Conflicts of Interest

The authors declare no conflicts of interest regarding the publication of this paper.

References

[1] Nakamura, M., Yamaguchi, K., Kimoto, Y., Yasaki, Y., Kato, T. and Sugimoto, H. (2019) Cd-Free Cu(In,Ga)(Se,S)$_2$ Thin-Film Solar Cell with Record Efficiency of 23.35%. *IEEE Journal of Photovoltaics*, **9**, 1863-1867. https://doi.org/10.1109/JPHOTOV.2019.2937218

[2] Aboulfadl, H., Keller, J., Larsen, J., Thuvander, M., Riekehr, L., Edoff, M. and Platzer-Björkman, C. (2019) Microstructural Characterization of Sulfurization Effects in Cu(In,Ga)Se$_2$ Thin Film Solar Cells. *Microscopy and Microanalysis*, **25**, 532-538. https://doi.org/10.1017/S1431927619000151

[3] Sylla, A., Touré, S. and Vilcot, J.-P. (2017) Numerical Modeling and Simulation of CIGS-Based Solar Cells with ZnS Buffer Layer. *Open Journal of Modelling and Simulation*, **5**, 218-231. https://doi.org/10.4236/ojmsi.2017.54016

[4] Sylla, A., Touré, S. and Vilcot, J.-P. (2017) Theoretical Analysis of the Effects of Band Gaps and the Conduction Band Offset of ZnS-CIGS Layers, as Well as Defect Layer Thickness. *International Journal of Science and Research*, **6**, 855-861. https://www.ijsr.net/search_index_results_paperid.php?id=ART20178061

[5] Wei, S.-H., Zhang, S.B. and Zunger, A. (1998) Effects of Ga Addition to CuInSe$_2$ on Its Electronic, Structural, and Defect Properties. *Applied Physics Letters*, **72**, 3199-3201. https://doi.org/10.1063/1.121548

[6] Wei, S.-H. and Zunger, A. (1995) Band Offsets and Optical Bowings of Chalcopyrites and Zn-Based II-VI Alloys. *Journal of Applied Physics*, **78**, 3846-3856. https://doi.org/10.1063/1.359901

[7] Mudryi, A.V., Gremenok, V.F., Karotki, A.V., Zalesski, V.B., Yakushev, M.V., Luckert, F. and Martin, R. (2010) Structural and Optical Properties of Thin Films of Cu(In,Ga)Se$_2$ Semiconductor Compounds. *Journal of Applied Spectroscopy*, **77**, 371-377. https://doi.org/10.1007/s10812-010-9341-5

[8] Ahn, B.T., Larina, L., Kim, K.H. and Ahn, S.J. (2008) Development of New Buffer Layers for Cu(In,Ga)Se$_2$ Solar Cells. *Pure and Applied Chemistry*, **80**, 2091-2102. https://doi.org/10.1351/pac200880102091

[9] Pettersson, J. (2012) Modeling Band Gap Gradients and Cd-Free Buffer Layers in Cu(In,Ga)Se$_2$ Solar Cells. Ph.D. Thesis, Uppsala University, Uppsala. https://www.diva-portal.org/smash/get/diva2:501452/FULLTEXT01.pdf

[10] Meyer, B.K., Polity, A., Farangis, B., He, Y., Hasselkamp, D., Krämer, T. and Wang, C. (2004) Structural Properties and Band Gap Bowing of $ZnO_{1-x}S_x$ Thin Films Deposited by Reactive Sputtering. *Applied Physics Letters*, **85**, 4929-4931. https://doi.org/10.1063/1.1825053

[11] Decocka, K., Lauwaerta, J. and Burgelmana, M. (2010) Characterization of Graded CIGS Solar Cells. *Energy Procedia*, **2**, 49-54.

https://doi.org/10.1016/j.egypro.2010.07.009

[12] Orgassa, K., Schock, H.W. and Werner, J.H. (2003) Alternative Back Contact Materials for Thin-Film Cu(In,Ga)Se Solar Cells. *Thin Solid Films*, **431-432**, 387-391. https://doi.org/10.1016/S0040-6090(03)00257-8

[13] Matson, R.J., Jamjoum, O., Buonaquisti, A.D., Russell, P.E., Kazmerski, L.L., Sheldon, P. and Ahrenkiel, R.K. (1984) Metal Contacts to $CuInSe_2$. *Solar Cells*, **11**, 301-305. https://doi.org/10.1016/0379-6787(84)90019-X

[14] Assmann, L., Bernède, J.C., Drici, A., Amory, C., Halgand, E. and Morsli, M. (2005) Study of the Mo Thin Films and Mo/CIGS Interface Properties. *Applied Surface Science*, **246**, 159-166. https://doi.org/10.1016/j.apsusc.2004.11.020

[15] Lide, D.R. (2005) CRC Handbook of Chemistry and Physics. Internet Version, CRC Press, Boca Raton, 2208. http://www.hbcpnetbase.com

[16] Klinkert, T., Theys, B., Patriarche, G., Jubault, M., Donsanti, F., Guillemoles, J.-F. and Lincot, D. (2016) New Insights into the Mo/Cu(In,Ga)Se_2 Interface in Thin Film Solar Cells: Formation and Properties of the $MoSe_2$ Interfacial Layer. *The Journal of Chemical Physics*, **145**, Article ID: 154702. https://doi.org/10.1063/1.4964677

[17] Kohara, N., Nishiwaki, S., Hashimoto, Y., Negami, T. and Wada, T. (2001) Electrical Properties of the Cu(In,Ga)Se_2/$MoSe_2$/Mo Structure. *Solar Energy Materials & Solar Cells*, **67**, 209-215. https://doi.org/10.1016/S0927-0248(00)00283-X

[18] Hsiao, K.-J., Liu, J.-D., Hsieh, H.-H. and Jiang, T.-S. (2013) Electrical Impact of $MoSe_2$ on CIGS Thin-Film Solar Cells. *Physical Chemistry Chemical Physics*, **41**, 18174-18178. https://doi.org/10.1039/c3cp53310g

[19] Wada, T., Kohara, N., Nishiwaki, S. and Negami, T. (2001) Characterization of the Cu(In,Ga)Se_2/Mo interface in CIGS. *Thin Solid Films*, **387**, 118-122. https://doi.org/10.1016/S0040-6090(00)01846-0

[20] Zhang, X., Kobayashi, M. and Yamada, A. (2017) Comparison of Ag(In,Ga)Se_2/Mo and Cu(In,Ga)Se_2/Mo interfaces in solar cells. *ACS Applied Materials & Interfaces*, **9**, 16215-16220. https://doi.org/10.1021/acsami.7b02548

[21] Varache, R., Leendertz, C., Gueunier-Farret, M.E., Haschke, J., Muñoz, D. and Korte, L. (2015) Investigation of Selective Junctions Using a Newly Developed Tunnel Current Model for Solar Cell Applications. *Solar Energy Materials & Solar Cells*, **141**, 14-23. https://doi.org/10.1016/j.solmat.2015.05.014